

Contextual Causal Bayesian Optimisation

Vahan Arsenyam¹ Antoine Grosnit² Haitham Bou-Amor³

Abstract

Causal Bayesian Optimisation (CaBO) combines causality with Bayesian optimisation (BO) to address scenarios where neglecting causal knowledge leads to suboptimal outcomes. Despite its promise, CaBO lacks theoretical guarantees, particularly high-probability bounds on regret. This work bridges this gap by providing the first probabilistic regret bound for CaBO. While CaBO identifies controllable variables for intervention, it overlooks purely observational variables, limiting its ability to achieve the optimal regret. Building on the connections between CaBO and multi-armed bandits (MAB), which we establish in this paper, we propose a novel framework for contextual causal Bayesian optimisation. Our framework employs an upper confidence bound MAB (MAB-UCB) approach to efficiently determine the optimal combination of controlled and contextual variables, referred to as the policy scope. We show failure cases for existing methods, such as CaBO and contextual BO (CoBO), highlighting their inability to achieve optimal outcomes in certain scenarios. Empirical evaluations in diverse environments demonstrate that our framework achieves sub-linear regret, even in cases where other methods fail, and reduces sample complexity in high-dimensional environments.

1. Introduction

Bayesian optimisation (BO) (Garnett, 2023) is a widely-used machine learning technique for finding the optimum of expensive black-box functions. It is particularly efficient in scenarios where function evaluations are costly. Causal relationships often exist among controllable variables, which can be captured by a causal graph. In its standard form, BO ignores these relations and considers only a fixed set of controlled variables which results in sub-optimal solutions (Lee

& Bareinboim, 2018). A naive approach to test all subsets of controllable variables in a brute-force way becomes computationally prohibitive as the number of subsets to consider grows exponentially with the number of variables.

The line of work on causal Bayesian optimisation assumes that the causal graph is available and develops specific tools to exploit the graph and achieve lower regret than standard BO. Most recent work, named Causal Bayesian Optimisation (CaBO) (Aglietti et al., 2020), focuses on identifying the subset of controllable variables and the optimal intervention values for those variables to optimise the expectation of the target variable exploiting results from (Lee & Bareinboim, 2019). While CaBO demonstrates promising empirical results, it lacks theoretical performance guarantees. This paper addresses this gap by providing a high-probability regret bound. Similar to CaBO, we assume access to the causal graph, but if it is unavailable, extensive causal discovery literature (Spirtes et al., 2000; Hoyer et al., 2008; Hyttinen et al., 2013) provides methods for inferring it. Consistent with prior work (Aglietti et al., 2020; Zhang & Bareinboim, 2022), we consider only precise interventions (Pearl, 2009a).

We show that incorporating contextual information from non-interventional variables enhances the selection of intervention values. This contextual policy (distributions mapping from contexts to controlled variables) optimisation framework has applications across various fields, including engineering (Anderson, 1995; Partanen & Bitmead, 1993; Mills et al., 1991), economy (Hota & Sundaram, 2021), robotics (Gu et al., 2017), biology, and healthcare (Magill & Ray, 2009; Goldman-Mazur et al., 2022). Contextual Bayesian optimisation (CoBO) is a generalisation of standard Bayesian optimisation for scenarios where context is critical. CoBO informs its decision on which point to evaluate next by considering the current context of the black-box function. For instance, Baheri and Vermillion (2020) utilise CoBO to tune wind energy systems. Similarly, Fiducioso et al. (2019) apply a constrained version of CoBO to achieve sustainable room temperature control. Pinsler et al. (2019) and Feng et al. (2020) demonstrate the importance of using context information for data-efficient decision making by tuning contextual policies in a reinforcement learning setting. Likewise, Fauvel and Chalk (2021) emphasise the importance of contextualised strategies for adaptive optimi-

¹CREST, ENSAE, IP Paris, France ²TU Darmstadt, Germany

³Huawei Noah's Ark Lab, UK. Correspondence to: Vahan Arsenyan <vahan.arsenyan@ensae.fr>.

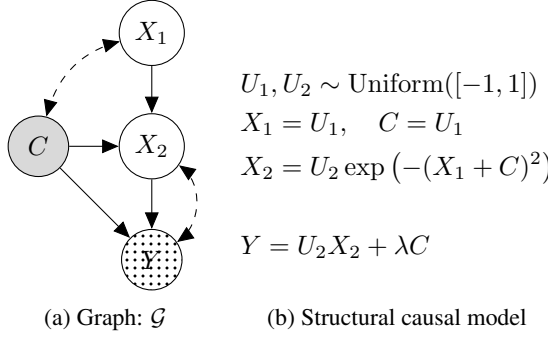


Figure 1. A toy illustration depicting a failure mode of contextual Bayesian optimisation. Fig. 1a presents the dependence or causal graph, and Fig. 1b shows the compatible structural model. The variables X_1 and X_2 are controllable, C represents a context variable, and Y is the objective variable to be maximised. U_1 and U_2 are two unobserved random variables independently sampled from a uniform distribution.

sation in psychometric measurements.

Although widely spread and commonly used, CoBO learns contextualised policies assuming fixed action and state spaces, whereby it *a priori* bears a prespecified set of interventional (optimisable) and contextual variables, respectively. We generally refer to tuple of interventional and contextual variables as a policy scope. However, when the policy scope is fixed, *CoBO can suffer from provably linear regret*, particularly when all controllable and contextual variables are included, as is often the case in practice.

An example of CoBO/CaBO’s failure modes: We employ the semantical framework of structural causal models (SCM) (Pearl, 2009b) to describe data generating processes in this paper. An SCM M is a tuple $\langle \mathbf{V}, \mathbf{U}, \mathcal{F}, P(\mathbf{U}) \rangle$, where \mathbf{V} is a set of endogenous variables and \mathbf{U} is a set of exogenous variables. \mathcal{F} is a set of functions such that each $f_V \in \mathcal{F}$ decides values of an endogenous variable $V \in \mathbf{V}$ taking as argument a combination of other variables in the system. That is, $V \leftarrow f_V(\mathbf{PA}_V, \mathbf{U}_V)$, $\mathbf{PA}_V \subseteq \mathbf{V}$, $\mathbf{U}_V \subseteq \mathbf{U}$. The exogenous variables $U \in \mathbf{U}$ are mutually independent, and their values are drawn from the exogenous distribution $P(\mathbf{U})$. Consequently, the SCM M induces a joint distribution $P(\mathbf{V})$ over the endogenous variables \mathbf{V} , referred to as the observational distribution.

Using the definition of SCM, we illustrate a failure mode for both CaBO and CoBO. Consider the example in Fig. 1, where the context variable C affects a controllable variable X_2 and the target objective Y . The graph \mathcal{G} contains another controllable variable X_1 , which influences X_2 and is associated with the context C . λ is an arbitrary constant.

The agent’s goal is to determine a policy π that maximises the expected target objective, i.e., $\max_{\pi} \mathbb{E}_{\pi}[Y]$. First, we

note that there is a policy that achieves $1/3$ as the expected value of Y . We will demonstrate this shortly, but first, let us consider how CaBO identifies three sets of variables, which are treated as policy scopes $\{\emptyset, \{X_1\}, \{X_2\}\}$ where \emptyset represents the passive observation. Under passive observation we compute that the expected value of Y is $\mathbb{E}[Y] = 1/3\mathbb{E}[e^{-4U_1^2}]$ which is less than $1/3$. Now, if X_2 is controlled, it becomes independent of U_2 and the expected value of Y becomes 0. Lastly, the control of X_1 yields $\mathbb{E}_{\text{do}(X_1=x_1)}[Y] = 1/3\mathbb{E}[e^{-(x_1+U_1)^2}]$ which reaches the maximum when x_1 is equal to 0. However, this maximum $\mathbb{E}_{\text{do}(X_1=0)}[Y]$ is less than $1/3$.

We now analyse the behaviour of CoBO in this scenario. By design, CoBO’s policy is such that $\pi_{\text{CoBO}} \equiv \pi_{\text{CoBO}}(x_1, x_2|c)$, where X_1 and X_2 are jointly controlled based on the context observation C . Following this strategy with the given policy scope, we derive that: $\mathbb{E}_{\pi_{\text{CoBO}}}[Y] = \mathbb{E}_{\pi_{\text{CoBO}}}[U_2 X_2 + \lambda C] = 0$ since π_{CoBO} controls X_2 independently of U_2 .

Alternatively, if we select a policy scope where X_1 is controlled based on C , denoted by $\pi_s \equiv \pi(x_1|c)$, we obtain a more favourable solution. To demonstrate this, we begin by expanding the objective function as follows:

$$\mathbb{E}_{\pi_s}[Y] = \mathbb{E}_{\pi_s}[U_2^2] \mathbb{E}_{\pi_{\text{scope}}}[e^{-(X_1+C)^2}] + \mathbb{E}_{\pi_s}[\lambda C]$$

We can clearly see that the optimum is achieved when *only* X_1 is controlled and set to $-C$, whereby: $\mathbb{E}_{\pi_s}[Y] = 1/3 > \mathbb{E}_{\pi_{\text{CoBO}}}[Y]$. In other words, we see through this example that choosing the “wrong” scope may produce policies that do not achieve the sought optima.

The problem addressed in this paper arises naturally from the three key challenges identified above. These challenges are: (1) CoBO has to optimise over candidate policies with varying state-action spaces to determine optima. (2) As the number of contextual policy scopes grows exponentially with the number of variables, performing an exhaustive search becomes computationally infeasible. (3) CaBO fails when faced with contextual variables. To the best of our knowledge, no existing algorithm effectively addresses these challenges. In this paper, we propose the first technique for contextual and causal BO.

Our method, called CoCa-BO, is capable of reducing the search space of policy scopes without compromising the convergence to the optimum. We identify challenges associated with using the causal acquisition function (Aglietti et al., 2020) to select the optimal policy scope in a contextual setting. We propose a novel approach that effectively identifies the optimal policy scope and simplifies the selection process. We analytically demonstrate cases where other methods fail and experimentally show that CoCa-BO consistently converges to the optimum. Furthermore, our empirical results reveal a significant reduction in sample

complexity for large systems, even when other techniques can also achieve optimal solutions. We list our main contributions below:

- We prove the first probabilistic regret bound for a general class of problems, termed multi-function BO, from which the CaBO case follows as a special instance.
- We propose a novel method for context-aware causal Bayesian optimisation, inspired by our established connection between CaBO and MAB, that effectively overcomes the limitations of policy scope selection imposed by the causal acquisition function.
- We provide a general, scalable, and user-friendly framework for implementing causality-aware optimisation algorithms, along with a suite of environments for testing and benchmarking them.

2. Related Work

The application of causal knowledge to derive improved policies and policy scopes is a rapidly evolving research area (Lee & Bareinboim, 2018; 2019; 2020). Notable advancements have been made in deriving conditional and unconditional policies across various contexts (Aglietti et al., 2020; Zhang & Bareinboim, 2017; 2022). We describe these developments from both causal and Bayesian optimisation perspectives.

2.1. Causal BO

Causal Bayesian Optimisation (CaBO) (Aglietti et al., 2020) combines the theory of possible optimal minimal interventional sets (POMIS) (Lee & Bareinboim, 2018; 2019) with the BO framework. CaBO assumes a given causal graph, which may include unobserved confounders, and aims to identify a subset of interventional variables and their corresponding values to optimise the expectation of the target variable. Since the power set of interventional variables grows exponentially with their number, optimising over even moderate systems becomes infeasible. CaBO derives the set of POMISes (Lee & Bareinboim, 2018) from the causal graph and restricts its search space accordingly. A POMIS is defined as an optimal interventional set for any SCM consistent with the causal graph. Ignoring a POMIS implies the existence of an SCM where no alternative interventional set achieves the optimum. Lee & Bareinboim (2018) also show that in some cases, an agent intervening on all interventional variables, which is a standard case in BO, never achieves the optimum. CaBO effectively ignores non-controllable observed variables by projecting the original causal graph into a new one where these variables are treated as latent (Lee & Bareinboim, 2019). This procedure marginalises uncontrollable observed variables, simplifying

the model.

After computing POMISes, CaBO decides at each step which POMIS and which interventional values to suggest, and runs the corresponding black-box evaluation. To make this decision, CaBO maximises for each POMIS an acquisition function based on a causal Gaussian process (GP) (Rasmussen & Williams, 2006) model per POMIS. CaBO returns the POMIS and the corresponding interventional values that attained the largest acquisition function value overall. Once CaBO has performed the intervention on the system, it collects the value of the target variable, and updates the GP of the selected POMIS. Contrary to CaBO, our method exploits the contextual variables available to the agent, and performs a search over the joint space of interventional and contextual variables. Note that this space is a super-set of the POMISes set, therefore we observe that our method recovers CaBO optima in absence of contexts, and achieves better optima than CaBO when contextual information is essential for the decisions. We discuss the challenges of generalising CaBO to contextual scenarios, particularly the instabilities caused by acquisition function-based policy scope selection in contextual optimisation, in Section 5.2.

2.2. Contextual BO

An agent may achieve better optima by considering some observable variables as contextual ones. It should decide the values at which interventional variables are controlled based on the values of contextual variables. Contextual BO is an algorithm well suited for this scenario. A kernel function is defined on the product space of both contextual and interventional variables, but the acquisition function is optimised only over the controllable variables as the contextual ones are fixed by the system at each step.

The common way of utilising CoBO is to consider all controllable variables as interventional and other observed ones as contextual within the system. This may never recover the optimal policy (Lee & Bareinboim, 2020). Moreover, it may lead to slower convergence as the optimisation space grows exponentially with each variable. Compared to CoBO, the method we propose optimises over mixed policy scopes (Lee & Bareinboim, 2020) which allows our method to efficiently circumvent suboptimality of CoBO.

2.3. Reinforcement Learning for Mixed Policy Scopes

The work in (Zhang & Bareinboim, 2022) considers a setup where all endogenous variables are discrete, and exogenous ones can be discrete or continuous. The algorithm they propose is the causal-UCB* focusing on special policy scopes, that guarantee to contain the optimal one to reduce the search space. They show that in general, the bound for the causal-UCB* is smaller than the bound for the standard UCB, which demonstrates the importance of causal knowl-

edge for building efficient agents. This method limits itself to cases where all observable variables are discrete and have finite domains. Whereas our proposed solution works for both discrete and continuous variables.

3. Background

3.1. Preliminaries

We will denote the causal graph of the problem by \mathcal{G} , and the target variable that we should optimise by Y . Random variables will be denoted by capital letters like X and their values with corresponding lowercase letters like x . The domain of random variable X will be noted \mathfrak{X}_X . Sets of variables will be denoted by bold capital letters \mathbf{X} and the set of corresponding values by bold lowercase letters \mathbf{x} . Let \mathbf{V} denote the set of all the observable variables in the system. MPS is defined as:

Definition 3.1 (Mixed policy scopes (MPS)). Let $\mathbf{X}^* \subseteq \mathbf{V} \setminus \{Y\}$ be a set of interventional variables, and $\mathbf{C}^* \subseteq \mathbf{V} \setminus \{Y\}$ be a set of contextual variables. A mixed policy scope \mathcal{S} is defined as a collection of pairs $\langle X \mid \mathbf{C}_X \rangle$ such that $X \in \mathbf{X}^*$, $\mathbf{C}_X \subseteq \mathbf{C}^* \setminus \{X\}$. Additionally, $\mathcal{G}_{\mathcal{S}}$ is acyclic, where $\mathcal{G}_{\mathcal{S}}$ is \mathcal{G} with edges onto X removed and new ones added from \mathbf{C}_X to X for every $\langle X \mid \mathbf{C}_X \rangle \in \mathcal{S}$.

A policy based on the MPS \mathcal{S} is defined as:

Definition 3.2 (Policy of an MPS). Given $\langle \mathcal{G}, Y, \mathbf{X}^*, \mathbf{C}^* \rangle$ and an SCM \mathcal{M} conforming the graph \mathcal{G} with $\mathfrak{X}_Y \subseteq \mathbb{R}$, a mixed policy π is a realisation of a mixed policy scope \mathcal{S} compatible with the tuple $\pi \doteq \{\pi_{X \mid \mathbf{C}_X}\}_{\langle X, \mathbf{C}_X \rangle \in \mathcal{S}}$, where $\pi_{X \mid \mathbf{C}_X} : \mathfrak{X}_X \times \mathfrak{X}_{\mathbf{C}_X} \mapsto [0, 1]$ is a proper probability mapping.

We denote the space of policies that are compatible with an MPS \mathcal{S} by $\Pi_{\mathcal{S}}$, and the set of all mixed policy scopes is denoted by \mathbb{S} . We define $\Pi_{\mathbb{S}} = \bigcup_{\mathcal{S} \in \mathbb{S}} \Pi_{\mathcal{S}}$ as the space of all policies, $\mathbf{X}(\mathcal{S})$ designates the set of interventional variables for an MPS \mathcal{S} and $\mathbf{C}(\mathcal{S})$ the contextual ones.

Our goal is to find a policy $\pi^* \in \Pi_{\mathbb{S}}$ maximising the expected reward Y , i.e. $\pi^* = \operatorname{argmax}_{\pi \in \Pi_{\mathbb{S}}} \mathbb{E}_{\pi}[Y]$. In this paper, we make the standard assumption that the agent knows the causal graph \mathcal{G} but does not have access to the underlying SCM of the environment.

3.2. POMPS

Our work focuses on a special set of MPSes that are possibly optimal under an SCM compatible with \mathcal{G} .

Definition 3.3 (Possibly-Optimal MPS (POMPS)). Given $\langle \mathcal{G}, Y, \mathbf{X}^*, \mathbf{C}^* \rangle$. An MPS $\mathcal{S} \in \mathbb{S}$ is said to be possibly-optimal if there exists an SCM \mathcal{M} compatible with the graph \mathcal{G} such that $\mu_{\mathcal{S}}^* > \max_{\mathcal{S}' \in \mathbb{S} \setminus \mathcal{S}} \mu_{\mathcal{S}'}^*$.

It is impossible to further restrict the search space to a

Algorithm 1 Multi-function BO

```

1: Input: Input spaces  $\mathfrak{X}_i$ ; GP Prior  $\mu_0 = 0, \sigma, k_i$ 
2: for  $t = 1, 2, \dots$  do
3:    $i_t = \arg \max_{i \in \llbracket m \rrbracket} \max_{\mathbf{x}^{(i)} \in \mathfrak{X}_i} \mu_{t-1}^{(i)}(\mathbf{x}^{(i)}) + \sqrt{\beta_t} \sigma_{t-1}^{(i)}(\mathbf{x}^{(i)})$ 
4:    $\mathbf{x}_t = \arg \max_{\mathbf{x}^{(i_t)} \in \mathfrak{X}_{i_t}} \mu_{t-1}^{(i_t)}(\mathbf{x}^{(i_t)}) + \sqrt{\beta_t} \sigma_{t-1}^{(i_t)}(\mathbf{x}^{(i_t)})$ 
5:   Observe  $y_t = f_{i_t}(\mathbf{x}_t) + \epsilon_t$ 
6:   Perform Bayesian update to obtain  $\mu_t^{(i_t)}$  and  $\sigma_t^{(i_t)}$ 
7: end for

```

subset of \mathbb{S}^* *a priori*. Indeed, for each POMPS \mathcal{S} , there will always exist an SCM \mathcal{M} compatible with \mathcal{G} for which \mathcal{S} yields the optimum value. Therefore, knowing only \mathcal{G} , the agent cannot exclude a POMPS without the risk of missing the optimal policy. Before introducing our algorithm for the contextual case, we first analyse the performance of CaBO, as it highlights the link between CaBO and MAB, which we later exploit.

4. Regret Bound for CaBO

We derive a bound for a more general algorithm, which we refer to as multi-function BO, from which the CaBO case readily follows. Let $\mathfrak{X}_i \subset [0, r_i]^{d_i}$ be compact and convex where $d_i \in \mathbb{N}$ and $r_i > 0$ for $i \in \llbracket m \rrbracket$, where $\llbracket m \rrbracket$ denotes the set of integers i such that $1 \leq i \leq m$. Assume that $f_i \sim \mathcal{GP}(0, k_i(\mathbf{x}, \mathbf{x}'))$ defined on \mathfrak{X}_i . Let $k_i(\mathbf{x}, \mathbf{x}) \leq 1$ and $k_i(\mathbf{x}, \mathbf{x}')$ have fourth order mixed partial derivatives, where the conditions on k_i ensure the smoothness of sample paths (Ghosal & Roy, 2006). More formally, $\exists a_i, b_i \geq 0$ constants such that:

$$P \left(\sup_{\mathbf{x} \in \mathfrak{X}_i} \left| \frac{\partial f_i}{\partial x_j} \right| > L \right) \leq a_i e^{-(L/b_i)^2}, \quad j = 1, \dots, d_i.$$

Denote $\mathbf{x}_*^{(i)} = \arg \max_{\mathbf{x}^{(i)} \in \mathfrak{X}_i} f_i(\mathbf{x}^{(i)})$, $\nu_i = f_i(\mathbf{x}_*^{(i)})$, and $\nu^* = \max_{i \in \llbracket m \rrbracket} \nu_i$. We consider step-wise optimisation that aims to find ν^* as fast as possible. Schematically, at each step t , the algorithm under consideration chooses an index $i_t \in \llbracket m \rrbracket$ and a point of evaluation $\mathbf{x}_t \in \mathfrak{X}_{i_t}$. It then observes $y_{i_t} := f_{i_t}(\mathbf{x}_t) + \epsilon_t$, where $\epsilon_t \stackrel{\text{iid}}{\sim} \mathcal{N}(0, \sigma^2)$. We focus on the case where the selection rules are based on the upper confidence bounds of the corresponding GPs. The knowledge update follows the Bayesian posterior update for the chosen GP (see Algorithm 1) with $\mu_{t-1}^{(i)}$ and $\sigma_{t-1}^{(i)}$ denoting the posterior mean and covariance of the i^{th} GP at time t .

For our choice of i_t and \mathbf{x}_t , the instantaneous regret is defined as $r_t = \nu^* - f_{i_t}(\mathbf{x}_t)$, and the cumulative regret (henceforth referred to simply as regret) is $R_n = \sum_{t=1}^n r_t$. Notably, this definition of regret differs from those in the

multi-armed bandit (MAB) (Lattimore & Szepesvári, 2020) and Bayesian optimisation (BO) (Srinivas et al., 2010) literature. Unlike MAB, where the expected reward per “arm” i_t is constant, our expected reward evolves as the maxima of f_{i_t} are iteratively refined. Similarly, unlike BO, our regret compares the current estimate of the maxima of f_{i_t} to ν^* which may be an optimal value of a different function. These distinctions introduce additional challenges in deriving the high-probability bound for R_n of Algorithm 1.

Theorem 4.1. *Let $\delta \in (0, 1)$, $d = \max_i d_i$, $a = \max_i a_i$, $b = \max_i b_i$, $r = \max_i r_i$, $\gamma_n = \max_i \gamma_n^{(i)}$, $C = \frac{8}{\ln(1+\sigma^{-2})}$ then the following is true for R_n*

$$P\left(R_n \leq \sqrt{mnC\beta_n\gamma_n} + \pi^2/6 \quad \forall n \geq 1\right) \geq 1 - \delta$$

where $\beta_n = 2 \log\left(\frac{4\pi n}{\delta}\right) + 4d \log\left(ndbr\sqrt{\log\left(\frac{4da}{\delta}\right)}\right)$.

The $\gamma_n^{(i)}$ is the maximum information gain of the i^{th} GP over horizon n (Srinivas et al., 2010), and we refer to (Vakili et al., 2021) for the latest results on bounding the maximum information gain in terms of n and the kernel parameters. The regret for CaBO follows by simply setting m to be the number of POMISes for a given causal graph. The proof of our result is provided in Appendix A.

Each arm i is selected according to the expression $\max_{\mathbf{x}^{(i)} \in \mathfrak{X}_i} \mu_{t-1}^{(i)}(\mathbf{x}^{(i)}) + \sqrt{\beta_t} \sigma_{t-1}^{(i)}(\mathbf{x}^{(i)})$ which relies only on past observations from arm i . Thus, Algorithm 1 operates as an index algorithm (Lattimore & Szepesvári, 2020), which is a subclass of MAB algorithms. Furthermore, the regret bound in Theorem 4.1 resembles the MAB-UCB bound, $\mathcal{O}(\sqrt{nm \log n})$, given that β_n scales as $\log(n)$. The inclusion of the $\sqrt{\gamma_n}$ term results in a larger bound compared to that of MAB-UCB. This arises because Algorithm 1 must search for both the optimal arm i^* and for the optimal $\mathbf{x}^* \in \mathfrak{X}_{i^*}$. The complexity of the latter task is captured by the $\sqrt{\gamma_n}$ term (Srinivas et al., 2010; Krause & Ong, 2011). Our decision to employ MAB-UCB for POMPS optimization in Section 5 stems from the connection we identified between CaBO and MAB-UCB. Our method effectively overcomes the issue of causal acquisition function used in CaBO for contextual optimisation which we discuss in .

5. Proposed Solution

In this section, we first define the optimisation algorithm we propose. We then discuss the limitations of the causal acquisition function, which is used in CaBO, in a contextual setting. We design an alternative approach that is effective in identifying the optimal POMPS for the given task. To illustrate the challenges of aligning the causal acquisition function with a contextual setup, we provide an example that demonstrates the difficulties arising in such scenarios.

5.1. Contextual BO policy

We augment each POMPS \mathcal{S} with a contextual GP that models the black-box to optimise as a function of $\mathbf{C}(\mathcal{S})$ and $\mathbf{X}(\mathcal{S})$. We also keep track of all the points evaluated so far when \mathcal{S} was selected in a dataset $\mathcal{D}_{\mathcal{S}}^t = \{(\mathbf{x}_{\mathcal{S}}^i, \mathbf{c}_{\mathcal{S}}^i, \mathbf{y}^i)\}_{i \in t_{\mathcal{S}}}$ where $t_{\mathcal{S}} = \{i \leq t \text{ s.t. } \mathcal{S}_i = \mathcal{S}\}$. Each GP model is characterised by a prior mean μ and a contextual kernel k , which are designed to capture the behaviour of the objective function as context and intervention values vary. The GP associated to scope \mathcal{S} with dataset $\mathcal{D}_{\mathcal{S}}^t$ provides a posterior prediction of the output we would observe by applying interventions $\mathbf{x}_{\mathcal{S}}$ in context $\mathbf{c}_{\mathcal{S}}$, given by $\mathcal{N}(\mu_{\text{post}}(\mathbf{z}_{\mathcal{S}}), \sigma_{\text{post}}(\mathbf{z}_{\mathcal{S}})^2)$ where $\mathbf{z}_{\mathcal{S}} = (\mathbf{x}_{\mathcal{S}}, \mathbf{c}_{\mathcal{S}})$ and:

$$\begin{aligned} \mu_{\text{post}}(\mathbf{z}_{\mathcal{S}}) &= \mathbf{k}_{t_{\mathcal{S}}}^{\top}(\mathbf{z}_{\mathcal{S}}) (\mathbf{K}_{t_{\mathcal{S}}} + \sigma_n^2 \mathbf{I})^{-1} \mathbf{y}_{t_{\mathcal{S}}} \\ \sigma_{\text{post}}(\mathbf{z}_{\mathcal{S}})^2 &= k(\mathbf{z}_{\mathcal{S}}, \mathbf{z}_{\mathcal{S}}) \\ &\quad - \mathbf{k}_{t_{\mathcal{S}}}^{\top}(\mathbf{z}_{\mathcal{S}}) (\mathbf{K}_{t_{\mathcal{S}}} + \sigma_n^2 \mathbf{I})^{-1} \mathbf{k}_{t_{\mathcal{S}}}(\mathbf{z}_{\mathcal{S}}), \end{aligned}$$

with \mathbf{I} the identity matrix, $\mathbf{y}_{t_{\mathcal{S}}}$ the vector of all observed targets in $\mathcal{D}_{\mathcal{S}}^t$, $\mathbf{K}_{t_{\mathcal{S}}}$ the covariance matrix of all interventional values and context pairs in $\mathcal{D}_{\mathcal{S}}^t$, $\mathbf{k}_{t_{\mathcal{S}}}$ the vector of covariances between $\mathbf{z}_{\mathcal{S}}$ and each already evaluated inputs, and σ_n a tunable noise level.

In our method, we deploy HEBO (Cowen-Rivers et al., 2022) for each POMPS, as it is a state-of-the-art BO algorithm (Turner et al., 2021) capable of handling optimisation in contextual settings and accommodating both continuous and discrete variables. HEBO’s GP model integrates input and output learnable transformations, making it robust to potential heteroscedasticity and non-stationarity. These challenges are common in contextual environments, where a change of context may induce a regime change. Notably, we have incorporated the strengths of HEBO into the implementation of CaBO through our general framework. Consequently, all methods in Section 6 utilise the same BO routine.

5.2. POMPS selection

In contrast to our method, CaBO utilises the values of the acquisition function for each GP to decide which POMIS should be controlled next. The motivation for such an approach comes from the observation that the best POMIS with the best interventional values will have a higher value of the expectation of the target than the others, by definition. Consequently, the acquisition function should be able to capture this pattern, especially in regions of low uncertainty. Nevertheless, this approach is not applicable in contextual cases as the optimal values of the acquisition functions are dependent on the context observed. This leads to the comparison of different functions at different points, i.e. different contexts. For example, consider POMPSes \mathcal{S} and \mathcal{S}' for which $\mathbf{c}_{\mathcal{S}}$ and $\mathbf{c}_{\mathcal{S}'}$ context has been observed

correspondingly. The comparison of maximal acquisition function values associated with \mathcal{S} and $c_{\mathcal{S}}$ on the one hand, and with \mathcal{S}' and $c'_{\mathcal{S}'}$, on the other hand, are not reflective of the relation between $\mathbb{E}_{\pi_{\mathcal{S}}^*}[Y]$ and $\mathbb{E}_{\pi_{\mathcal{S}'}^*}[Y]$. It may even lead to the divergence of the optimiser as such comparison may switch between POMPSes depending on the observed context. One possible alternative is to treat policy scopes as an axis of optimisation for BO. However, since POMPSes define the optimisation variables and each one creates a distinct optimisation domain, this approach becomes impractical.

We adopt MAB with upper confidence bound (UCB) action selection criterion (Sutton & Barto, 2018). Each POMPS serves as an arm for the MAB-UCB, where it attempts to find the arm with the highest reward, which is the POMPS with the best $\mu_{\mathcal{S}}^*$. One may argue that for a given POMPS \mathcal{S} the $\mathbb{E}_{\pi_{\mathcal{S}}}[Y]$ is changing as the policy is being optimised. Nevertheless, note that under optimality, it is stationary and equal to $\mu_{\mathcal{S}}^*$.

Algorithm 2 Contextual Causal BO (CoCa-BO)

Input: causal graph \mathcal{G} , number of iterations n , set of interventional variables \mathbf{X} , domain of variables $\mathfrak{X}_{\mathbf{V}}$.
 Compute $\mathbb{S}^* = \text{POMPS}(\mathcal{G}, \mathbf{X})$
 Create $A = \text{MAB-UCB}(\mathbb{S}^*)$
for $\mathcal{S} \in \mathbb{S}^*$ **do**
 Create $\text{Opt}_{\mathcal{S}} = \text{HEBO}(\mathbf{X}(\mathcal{S}), \mathbf{C}(\mathcal{S}), \mathfrak{X}_{\mathcal{S}})$
end for
for $i = 1$ **to** n **do**
 Select a POMPS: $\mathcal{S} = A.\text{suggest}()$
 Implement $\pi_{\mathcal{S}}$ dictated by $\text{Opt}_{\mathcal{S}}$, $y, \mathbf{x}_{\mathcal{S}}, \mathbf{c}_{\mathcal{S}} \sim \mathcal{M}_{\pi_{\mathcal{S}}}$
 $A.\text{update}(y, \mathcal{S})$
 $\text{Opt}_{\mathcal{S}}.\text{update}(y, \mathbf{x}_{\mathcal{S}}, \mathbf{c}_{\mathcal{S}})$
end for

We outline our method in Algorithm 2. The POMPS function computes the set of POMPSes (Lee & Bareinboim, 2020) for a given causal graph \mathcal{G} and a set of interventional variables \mathbf{X} . Although the brute-force search over MPSes has a computational complexity of $\mathcal{O}(2^{|V|})$, this search is highly parallelisable, a feature we leverage in our implementation. We consider the set of all possible contextual variables as $\mathbf{V} \setminus \mathbf{X}$, which is sufficient for the optimal POMPS to not be missed¹.

MAB-UCB creates a UCB multi-armed bandit for choosing which POMPS to implement at iteration i . The selection is done by $\text{suggest}(\cdot)$ method call on the MAB-UCB. The first *for* loop initialises the HEBO optimisers for each POMPS \mathcal{S} based on its contextual $\mathbf{C}(\mathcal{S})$ variables, interventional $\mathbf{X}(\mathcal{S})$ variables, and the domain of all variables within \mathcal{S} denoted by $\mathfrak{X}_{\mathcal{S}}$. The last *for* loop implements the

policy $\pi_{\mathcal{S}}$ defined by $\text{Opt}_{\mathcal{S}}$ and collects the values under the policy. Next, both the MAB-UCB and the selected HEBO optimiser are updated with the observed values. These updates have a computational complexity of $\mathcal{O}(n^3)$ due to the Gaussian Process posterior updates, which involve matrix inversion of size n , where n is the number of iterations.

6. Experiments

We conduct a series of experiments to compare the proposed method with CaBO and CoBO. For each experiment and optimiser, we report the time-normalised cumulative regret $\bar{R}_t = \frac{1}{T} \sum_{t=1}^T \hat{r}_t$, where $\hat{r}_t = y_t - \mathbb{E}_{\pi^*}[Y]$ denotes the immediate pseudo-regret at iteration t . Additionally, we present the cumulative MPS selection frequency that indicates the fraction by which each MPS has been selected up to iteration t . In all experiments, HEBO optimiser instances are initialised with their default parameters (Cowen-Rivers et al., 2022).

Configuration I: Both the proposed method and the benchmark method can achieve the optimum. We aim to assess the additional cost introduced by the proposed method in terms of sample complexity. In environments with a large number of observed variables, CoBO results in an expansive optimisation domain, requiring a substantial number of samples. Our method leverages the independencies encoded within the causal graph to reduce the optimisation domain. For instance, in Appendix D, the dimensionality of the domain is reduced by a factor of 22.

Configuration II: The benchmark method cannot achieve the optimum. We practically confirm that there are cases where neither CoBO nor CaBO converges to the optimum, leading to linear cumulative regret. We also show that CoCa-BO converges to the optimum policy and has sub-linear cumulative regret.

We have conducted all experiments with 110 random seeds over 700 iterations, indicating that 700 distinct interventions have been implemented in the system. We have utilised a single-node compute system with 120 CPUs to fully exploit the parallelisation capabilities of our framework. However, the experiments can be replicated on a single-core machine with 16 GB of RAM. The results are presented as averages, with error bars representing 1.96 standard errors.

6.1. CaBO vs CoCa-BO

6.1.1. FIRST CONFIGURATION

The lack of contextual information in CaBO limits its potential to achieve optimal values. However, in cases where the context is deemed irrelevant parametrically, i.e. the SCM of the system is such that the optimal value of the target is the same across all values of the contextual variables (ho-

¹Per Lee & Bareinboim (2020) Proposition 2

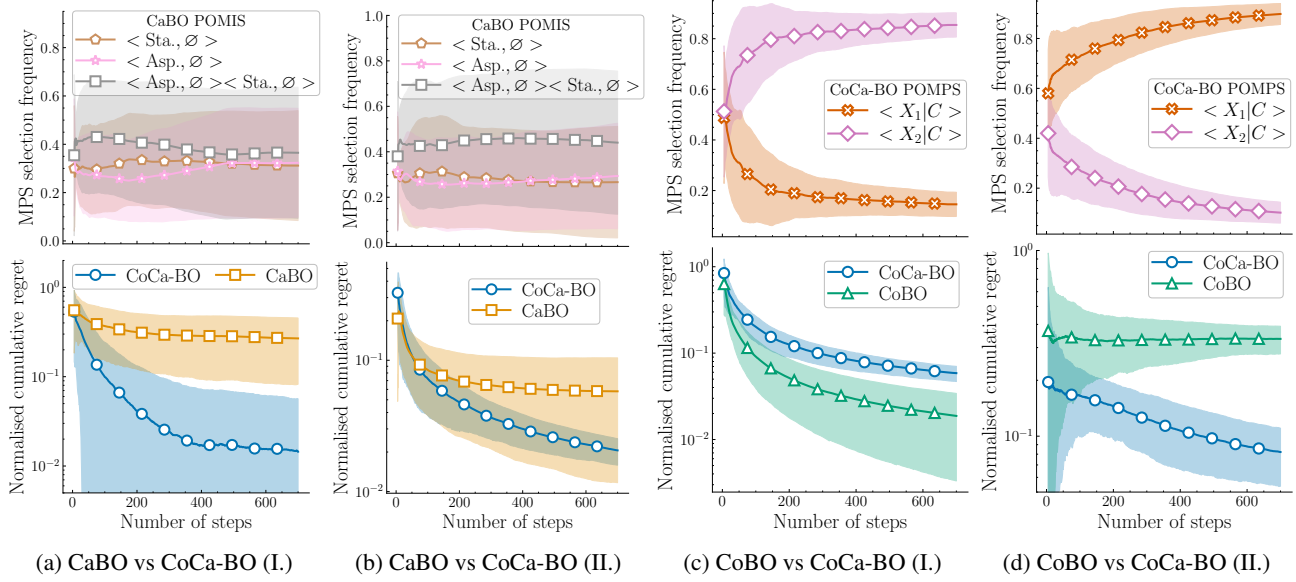


Figure 2. The upper figures show the cumulative probability of selecting the corresponding MPS (POMPS or POMIS). The frequency curve is omitted when there is only one candidate MPS. The lower charts show the time-normalised cumulative regret \bar{R}_T .

mogenous), CaBO is capable of attaining optima even in a contextual setup. However, these cases require a specific alignment of the SCM parameters, which may be unstable and can disappear even under small fluctuations (Pearl, 2009c). Another, less interesting, setup is when the contextual variables are in general irrelevant to the target Y which can be inferred from the causal graph \mathcal{G} . Our method is able to identify those cases and performs equally with CaBO as the set of POMPSes collapses to the set of POMISes in this case.

To further illustrate this, we define two SCMs that are compatible with the causal graph depicted in Fig. 3, from Ferro et al. (2015) (Ferro et al., 2015) and Thompson et al. (2019) (Thompson, 2019), where age, BMI, and cancer are only observable and aspirin, statin are interventional variables. PSA, which stands for prostate-specific antigen (Wang et al., 2011), is used to detect prostate cancer. We then compute the POMISes and POMPSes from the graph. The set of POMISes is $\{\emptyset, \{\text{Aspirin}\}, \{\text{Statin}\}, \{\text{Aspirin, Statin}\}\}$ and the set of POMPS consists of a single element, namely $\{\text{Aspirin, Statin} \mid \text{Age, BMI}\}$.

Under the parametrisation from (Aglietti et al., 2020), the optimal values at which Statin and Aspirin are controlled to minimise PSA are the same for all values of Age and BMI. Formally, the former statement can be written as $\forall(\text{age, bmi}) \in \mathfrak{X}_{\text{Age}} \times \mathfrak{X}_{\text{BMI}}$:

$$\begin{aligned} \operatorname{argmin}_{(\text{aspirin, statin})} \mathbb{E}[Y \mid \text{do}(\text{aspirin, statin}), \text{age, bmi}] \\ = \operatorname{argmin}_{(\text{aspirin, statin})} \mathbb{E}[Y \mid \text{do}(\text{aspirin, statin})] \end{aligned}$$

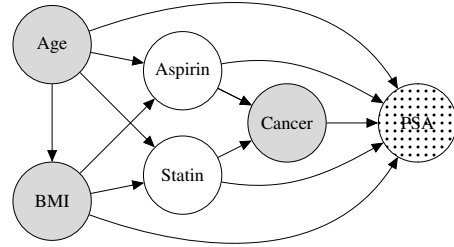


Figure 3. Causal graph of PSA level. White nodes represent variables which can be intervened and gray nodes represent non-manipulative variables. The target variable PSA is denoted with a shaded node.

We show that the optimal values at which Aspirin and Statin should be controlled at are 0 and 1 respectively (see Appendix B.1 for details).

Fig. 2a illustrates results for this setup. CaBO selects between POMISes following the causal acquisition function procedure. We note the high variance of this selection method, which practically harms the convergence properties of the optimiser. On the other hand, the MAB-UCB based POMPS selection of CoCa-BO practically does not suffer from this, as we see on Fig. 2c and Fig. 2d.

6.1.2. SECOND CONFIGURATION

The SCM for the second configuration is consistent with the causal graph in Fig. 3, and is such that if Aspirin and Statin are controlled based on Age and BMI, a lower expected

PSA is achieved than if Aspirin and Statin are controlled at constant values. Appendix B.2 shows that both Aspirin and Statin should both be controlled at $(\frac{\text{Age}-55}{21}) \mid \frac{\text{BMI}-27}{4}$ after plugging in Cancer equation into PSA, which entails that the optimal values for Aspirin and Statin depend on Age and BMI. CaBO cannot control medications based on Age and BMI as those contextual variables are marginalised, while our method converges as it utilises the $\langle \text{Aspirin}, \text{Statin} \mid \text{Age}, \text{BMI} \rangle$ and is able to identify a policy minimising PSA given Age and BMI.

Fig. 2b shows the results for this setup. We again observe high variance in the POMIS selection process for CaBO. The optimal policy being a contextual one renders it impossible for CaBO to achieve the optimum, yielding linear cumulative regret, as the normalised cumulative regret on Fig. 2b shows.

6.2. CoBO vs CoCa-BO

6.2.1. FIRST CONFIGURATION

Appendix C.1 describes an SCM consistent with the causal graph in Fig. 1a for which controlling both X_1 and X_2 does not impede the agent’s ability to achieve the optimal outcome. Fig. 2c shows that both methods converge to the optimal solution for this SCM, as evidenced by the decreasing trend of normalised cumulative regrets. We observe that CoBO actually converges faster than CoCa-BO. It is expected as CoBO optimises over a fixed policy scope, which reduces the cost associated with finding the optimal policy scope. Nevertheless, it is important to note that the convergence of CoBO is contingent on the specific parametric configuration of the SCM. Indeed, it is not possible to *a priori* exclude cases such as the one depicted in Fig. 1b, and therefore, it is necessary to perform a search over mixed policy sets (MPSes), or preferably over POMPSes, to enable convergence. Additionally, in environments with a large number of variables, CoBO performance deteriorates even if the convergence is still possible. We show in Appendix D that CoCa-BO converges significantly faster than CoBO in such settings due to its ability to identify and exclude irrelevant variables.

6.2.2. SECOND CONFIGURATION

The second configuration examined in this study is the SCM depicted in Fig. 1b in the introduction. We have shown analytically that the CoBO method is unable to attain the optimal solution. Our proposed method, CoCa-BO, has been demonstrated to effectively achieve the desired optimum, resulting in sub-linear cumulative regret. The upper sub-figure of Fig. 2d illustrates the cumulative probability of selecting the corresponding POMPS. Our proposed method, CoCa-BO, converges to the policy scope that yields the optimal value, specifically $\langle X_1 \mid C \rangle$. The lower sub-figure

of Fig. 2d illustrates that the normalised cumulative regret remains constant for CoBO, indicating its linear cumulative regret. On the other hand, our proposed method, CoCa-BO, attains sub-linear cumulative regret, as evidenced by the decreasing trend in the normalised cumulative regret corresponding to CoCa-BO.

6.3. Robustness to Noise

The target variable Y plays a pivotal role, as its observed values guide both policy scope and policy selection optimisation. Consequently, higher noise levels in Y lead to slower convergence rates for optimisation algorithms (Lattimore & Szepesvári, 2020; Krause & Ong, 2011; Srinivas et al., 2010).

To evaluate the robustness of CoCa-BO to noise in Y , we vary the standard deviation of ϵ_Y in the CoBO vs. CoCa-BO example (Appendix C.1), where the optimal value $\mathbb{E}_\pi[Y] = 1$ is achieved under the policy controlling $X_2 = C$. Specifically, $\sigma(\epsilon_Y)$ is adjusted from 0.01 to 6.25. As shown in Figure 5, CoCa-BO maintains convergence patterns even under extreme noise levels, such as $\sigma(\epsilon_Y) = 6.25$, which is 6.25 times the optimal target expectation (Appendix E).

7. Conclusion

In this paper, we reviewed Bayesian optimisation methods adapted to incorporate causal knowledge for achieving optimal results. We addressed concerns regarding the theoretical guarantees of CaBO by proving an upper bound on its regret. We have shown that existing methods struggle to incorporate non-interventional variables as context, often resulting in sub-optimal outcomes or exponentially high sample and computational costs. Additionally, we highlighted the connection between CaBO and multi-armed bandit (MAB) algorithms, both in terms of design and theoretical properties. To address these limitations, we introduced CoCa-BO, a new method that efficiently optimises policies in mixed policy scopes. Our analysis demonstrates that CoCa-BO consistently outperforms CaBO and CoBO, achieving optimal results across various environments. Notably, CoCa-BO reduces sample complexity in scenarios with large parameter spaces by identifying smaller optimisation domains without sacrificing convergence. Furthermore, CoCa-BO shows lower variance compared to CaBO, consistently reaching the optimum across multiple runs. We also share our PyRo-based code (Bingham et al., 2018; Phan et al., 2019) to facilitate reproducibility and provide a unified framework for future research in this domain.

Impact Statement

This paper presents work whose goal is to advance the field of Machine Learning. There are many potential societal

consequences of our work, none which we feel must be specifically highlighted here.

References

Aglietti, V., Lu, X., Paleyes, A., and González, J. Causal Bayesian optimization. *International Conference on Artificial Intelligence and Statistics*, pp. 3155–3164, 6 2020.

Anderson, B. D. Topical challenges of control engineering. *IFAC Proceedings Volumes*, 28(17):1–7, 1995. ISSN 1474-6670. 8th IFAC Symposium on Automation in Mining, Mineral and Metal Processing 1995 (MMM'95), Sun City, South Africa, 29-31 August.

Baheri, A. and Vermillion, C. Waypoint Optimization Using Bayesian Optimization: A Case Study in Airborne Wind Energy Systems. *2020 American Control Conference (ACC)*, 7 2020.

Bingham, E., Chen, J. P., Jankowiak, M., Obermeyer, F., Pradhan, N., Karaletsos, T., Singh, R., Szerlip, P., Horsfall, P., and Goodman, N. D. Pyro: Deep Universal Probabilistic Programming. *Journal of Machine Learning Research*, 2018.

Chowdhury, S. R. and Gopalan, A. On kernelized multi-armed bandits. In Precup, D. and Teh, Y. W. (eds.), *Proceedings of the 34th International Conference on Machine Learning*, volume 70 of *Proceedings of Machine Learning Research*, pp. 844–853. PMLR, 06–11 Aug 2017. URL <https://proceedings.mlr.press/v70/chowdhury17a.html>.

Cowen-Rivers, A., Lyu, W., Tutunov, R., Wang, Z., Grosnit, A., Griffiths, R.-R., Maravel, A., Hao, J., Wang, J., Peters, J., and Bou Ammar, H. Hebo: Pushing the limits of sample-efficient hyperparameter optimisation. *Journal of Artificial Intelligence Research*, 74, 07 2022.

Fauvel, T. and Chalk, M. Contextual bayesian optimization with binary outputs. *ArXiv*, abs/2111.03447, 2021.

Feng, Q., Letham, B., Mao, H., and Bakshy, E. High-Dimensional Contextual Policy Search with Unknown Context Rewards using Bayesian Optimization. *Neural Information Processing Systems*, 33:22032–22044, 1 2020.

Ferro, A., Pina, F., Severo, M., Dias, P., Botelho, F., and Lunet, N. Use of statins and serum levels of Prostate Specific Antigen. *Acta Urológica Portuguesa*, 7 2015.

Fiducioso, M., Curi, S., Schumacher, B., Gwerder, M., and Krause, A. Safe Contextual Bayesian Optimization for Sustainable Room Temperature PID Control Tuning. *Proceedings of the Twenty-Eighth International Joint Conference on Artificial Intelligence*, 8 2019.

Garnett, R. *Bayesian Optimization*. Cambridge University Press, 2023. to appear.

Ghosal, S. and Roy, A. Posterior consistency of Gaussian process prior for nonparametric binary regression. *The Annals of Statistics*, 34(5):2413 – 2429, 2006. doi: 10.1214/009053606000000795. URL <https://doi.org/10.1214/009053606000000795>.

Goldman-Mazur, S., Visram, A., Rajkumar, S. V., Kapoor, P., Dispenzieri, A., Lacy, M. Q., Gertz, M. A., Buadi, F. K., Hayman, S. R., Dingli, D., Kourtelis, T., Gonsalves, W., Warsame, R., Muchtar, E., Leung, N., Kyle, R. A., and Kumar, S. K. Second- and third-line treatment strategies in multiple myeloma: a referral-center experience. *Blood Cancer Journal*, 12(12):164, 2022.

Gu, S., Holly, E., Lillicrap, T., and Levine, S. Deep reinforcement learning for robotic manipulation with asynchronous off-policy updates. In *2017 IEEE International Conference on Robotics and Automation (ICRA)*, pp. 3389–3396. IEEE Press, 2017.

Hota, A. R. and Sundaram, S. Controlling Human Utilization of Failure-Prone Systems via Taxes. *IEEE Transactions on Automatic Control*, 66(12):5772–5787, 12 2021.

Hoyer, P. O., Janzing, D., Mooij, J. M., Peters, J., and Schölkopf, B. Nonlinear causal discovery with additive noise models. *Neural Information Processing Systems*, 21:689–696, 12 2008.

Hyttinen, A., Eberhardt, F., and Hoyer, P. O. Experiment selection for causal discovery. *Journal of Machine Learning Research*, 14(1):3041–3071, 1 2013.

Koller, D. and Friedman, N. *Probabilistic Graphical Models: Principles and Techniques*. Adaptive computation and machine learning. MIT Press, 2009. ISBN 9780262013192.

Krause, A. and Ong, C. Contextual gaussian process bandit optimization. In Shawe-Taylor, J., Zemel, R., Bartlett, P., Pereira, F., and Weinberger, K. (eds.), *Advances in Neural Information Processing Systems*, volume 24. Curran Associates, Inc., 2011. URL https://proceedings.neurips.cc/paper_files/paper/2011/file/f3f1b7fc5a8779a9e618e1f23a7b7860-Paper.pdf.

Lattimore, T. and Szepesvári, C. *Bandit Algorithms*. Cambridge University Press, 2020.

Lee, S. and Bareinboim, E. Structural causal bandits: where to intervene? *Neural Information Processing Systems*, 31:2573–2583, 12 2018.

Lee, S. and Bareinboim, E. Structural Causal Bandits with Non-Manipulable Variables. *Proceedings of the AAAI Conference on Artificial Intelligence*, 33(01):4164–4172, 7 2019.

Lee, S. and Bareinboim, E. Characterizing Optimal Mixed Policies: Where to Intervene and What to Observe. *Neural Information Processing Systems*, 33:8565–8576, 1 2020.

Magill, M. and Ray, L. A. Cognitive-Behavioral Treatment With Adult Alcohol and Illicit Drug Users: A Meta-Analysis of Randomized Controlled Trials. *Journal of Studies on Alcohol and Drugs*, 70(4):516–527, 7 2009.

Mills, P. M., Lee, P. L., and McIntosh, P. A practical study of adaptive control of an alumina calciner. *Autom.*, 27: 441–448, 1991.

Partanen, A. and Bitmead, R. Excitation Versus Control Issues in Closed Loop Identification of Plant Models for a Sugar Cane Crushing Mill 1. *IFAC Proceedings Volumes*, 26(2):121–124, 7 1993.

Pearl, J. *Causality: Models, Reasoning and Inference*. Cambridge University Press, 2nd edition, 9 2009a.

Pearl, J. Causality: Models, Reasoning and Inference. chapter 7, pp. 201–215. Cambridge University Press, 2009b.

Pearl, J. Causality: Models, Reasoning and Inference. chapter 2, pp. 47–58. Cambridge University Press, 2009c.

Pearl, J. Causality: Models, Reasoning and Inference. chapter 1, pp. 26–36. Cambridge University Press, 2009d.

Phan, D., Pradhan, N., and Jankowiak, M. Composable effects for flexible and accelerated probabilistic programming in numpyro. *arXiv preprint arXiv:1912.11554*, 2019.

Pinsler, R., Karkus, P., Kupcsik, A., Hsu, D., and Lee, W. S. Factored Contextual Policy Search with Bayesian optimization. *2019 International Conference on Robotics and Automation (ICRA)*, 5 2019.

Rasmussen, C. E. and Williams, C. K. I. *Gaussian processes for machine learning*. Adaptive computation and machine learning. MIT Press, 2006. ISBN 026218253X.

Spirites, P., Glymour, C., and Scheines, R. *Causation, Prediction, and Search*. MIT press, 2nd edition, 2000.

Srinivas, N., Krause, A., Kakade, S., and Seeger, M. Gaussian process optimization in the bandit setting: no regret and experimental design. In *Proceedings of the 27th International Conference on International Conference on Machine Learning*, ICML’10, pp. 1015–1022, Madison, WI, USA, 2010. Omnipress. ISBN 9781605589077.

Sutton, R. S. and Barto, A. G. *Reinforcement Learning: An Introduction*. The MIT Press, second edition, 2018.

Thompson, C. Causal graph analysis with the causalgraph procedure. 2019.

Turner, R., Eriksson, D., McCourt, M., Kiili, J., Laaksonen, E., Xu, Z., and Guyon, I. Bayesian optimization is superior to random search for machine learning hyperparameter tuning: Analysis of the black-box optimization challenge 2020. In Escalante, H. J. and Hofmann, K. (eds.), *Proceedings of the NeurIPS 2020 Competition and Demonstration Track*, volume 133 of *Proceedings of Machine Learning Research*, pp. 3–26. PMLR, 06–12 Dec 2021.

Vakili, S., Khezeli, K., and Picheny, V. On information gain and regret bounds in gaussian process bandits. In Banerjee, A. and Fukumizu, K. (eds.), *Proceedings of The 24th International Conference on Artificial Intelligence and Statistics*, volume 130 of *Proceedings of Machine Learning Research*, pp. 82–90. PMLR, 13–15 Apr 2021. URL <https://proceedings.mlr.press/v130/vakili21a.html>.

Wang, X., Zhao, M., Nolte, D. D., and Ratliff, T. L. Prostate specific antigen detection in patient sera by fluorescence-free BioCD protein array. *Biosensors and Bioelectronics*, 26(5):1871–1875, 1 2011.

Zhang, J. and Bareinboim, E. Transfer Learning in Multi-Armed Bandit: A Causal Approach. *Adaptive Agents and Multi-Agents Systems*, pp. 1778–1780, 5 2017.

Zhang, J. and Bareinboim, E. Online reinforcement learning for mixed policy scopes. In Oh, A. H., Agarwal, A., Belgrave, D., and Cho, K. (eds.), *Advances in Neural Information Processing Systems*, 2022.

A. Proof of Theorem 4.1

This section describes the proof of Theorem 4.1. We employ strategy similar to (Srinivas et al., 2010; Vakili et al., 2021; Chowdhury & Gopalan, 2017) but we face additional challenges, namely our regret definition drastically differs from the one analysed in the GP bandit setups and we need to control high probability bounds induced by concentration inequalities for functions samples from different GPs.

We start from an inequality (Srinivas et al., 2010) for a standard Gaussian random variable $r \sim \mathcal{N}(0, 1)$.

$$P(r > c) \leq \frac{e^{-c^2/2}}{2}$$

Noting that for a $i \in \llbracket m \rrbracket$ and a point $\mathbf{x}^{(i)} \in \mathfrak{X}_i$, $f_i(\mathbf{x}^{(i)})$ is normally distributed with mean $\mu_{t-1}^{(i)}(\mathbf{x}^{(i)})$ and variance $\sigma_{t-1}^{(i)}(\mathbf{x}^{(i)})$ as f_i is sampled from the GP with posterior mean $\mu_{t-1}^{(i)}$ and variance $\sigma_{t-1}^{(i)}$. Applying the aforementioned concentration inequality for a standard Gaussian random variable with a union bound to $(f_i(\mathbf{x}^{(i)}) - \mu_{t-1}^{(i)}(\mathbf{x}^{(i)})) / \sigma_{t-1}^{(i)}(\mathbf{x}^{(i)})$ yields that

$$P\left(\left|f_i(\mathbf{x}^{(i)}) - \mu_{t-1}^{(i)}(\mathbf{x}^{(i)})\right| \leq \sqrt{\beta_t} \sigma_{t-1}^{(i)}(\mathbf{x}^{(i)})\right) \geq 1 - e^{-\beta_t/2} \quad (1)$$

Given that k_{i^*} has fourth order mixed partial derivatives, f^* satisfies the requirements of (Srinivas et al., 2010) Lemma 5.7. Hence, for $\delta \in (0, 1)$ and $\beta_t = 2 \log(2\pi_t/\delta) + 4d_{i^*} \log(td_{i^*} b_{i^*} r_{i^*} \sqrt{\log(2d_{i^*} a_{i^*}/\delta)})$, where $\pi_t > 0$ and $\sum_{t \geq 1} \pi_t = 1$, we have:

$$P\left(\left|f^*(\mathbf{x}^*) - \mu_{t-1}^*([\mathbf{x}^*]_t)\right| \leq \sqrt{\beta_t} \sigma_{t-1}^*([\mathbf{x}^*]_t) + \frac{1}{t^2}\right) \geq 1 - \delta; \quad \forall t \geq 1 \quad (2)$$

where $[\mathbf{x}^*]_t$ is the closest point to \mathbf{x}^* for a discretisation of \mathfrak{X}^* with parameter $\tau_t = t^2 d_{i^*} b_{i^*} r_{i^*} \sqrt{\log(2d_{i^*} a_{i^*}/\delta)}$. However, as β_t is a parameter of the algorithm it cannot depend on the unknown i^* . For that reason we take $a = \max a_i$, $b = \max b_i$, $r = \max r_i$, $d = \max d_i$ and $\beta_t = 2 \log(2\pi_t/\delta) + 4d \log(tdbr \sqrt{\log(4da/\delta)})$ noting that it is greater or equal to the previously defined β_t so it preserves the inequality.

We need to prove a high probability bound on the instantaneous regret at t :

Lemma A.1. *Let $\delta \in (0, 1)$ and $\beta_t = 2 \log(4\pi_t/\delta) + 4d \log(tdbr \sqrt{\log(4da/\delta)})$, then*

$$P\left(r_t \leq 2\sqrt{\beta_t} \sigma_{t-1}^{(i_t)}(\mathbf{x}_t) + 1/t^2\right) \geq 1 - \delta \quad \forall t \geq 1$$

Proof. We want inequality 1 to hold for all $t \geq 1$ with probability at least $1 - \delta/2$ for which we need $\beta_t \geq 2 \ln(2\pi_t/\delta)$. We also want inequality 2 to hold with probability at least $1 - \delta/2$ so they hold together with probability at least $1 - \delta$. Note that our choice of β_t meets conditions of both inequalities.

By definition $r_t = f^*(\mathbf{x}^*) - f^{(i_t)}(\mathbf{x}_t)$. Equation 2 implies that

$$f^*(\mathbf{x}^*) \leq \mu_{t-1}^*([\mathbf{x}^*]_t) + \sqrt{\beta_t} \sigma_{t-1}^*([\mathbf{x}^*]_t) + \frac{1}{t^2}$$

$\mu_{t-1}^*([\mathbf{x}^*]_t) + \beta_t^{1/2} \sigma_{t-1}^*([\mathbf{x}^*]_t) \leq \mu_{t-1}^{(i_t)}(\mathbf{x}_t) + \beta_t^{1/2} \sigma_{t-1}^{(i_t)}(\mathbf{x}_t)$ as i_t is chosen by maximising the upper confidence bound with β_t coefficient. Combining last two inequalities and Equation 1 we get:

$$r_t \leq \mu_{t-1}^{(i_t)}(\mathbf{x}_t) + \beta_t^{1/2} \sigma_{t-1}^{(i_t)}(\mathbf{x}_t) + \frac{1}{t^2} - f^{(i_t)}(\mathbf{x}_t) \leq 2\sqrt{\beta_t} \sigma_{t-1}^{(i_t)}(\mathbf{x}_t) + \frac{1}{t^2} \quad (3)$$

with probability $\geq 1 - \delta$

□

Now we may begin the proof of the main result.

Proof. Denote u_i to be the number of times i is played over the horizon n under Algorithm 1. Then the regret can be rewritten in the following way:

$$R_n = \sum_{t=1}^n r_t = \sum_{i=1}^m \sum_{j=1}^{u_i} r_j^{(i)}$$

where $r_j^{(i)}$ is the regret of i at j th play. We derive that

$$\sum_{t=1}^n 4\beta_t \sigma_{t-1}^{2;(i)}(\mathbf{x}_t) \leq 4\beta_n \sum_{i=1}^m \sum_{j=1}^{u_i} \sigma_{(j-1)}^{2;(i)} \leq \beta_n C \sum_{i=1}^m \gamma_{u_i}^{(i)} \leq C\beta_n \sum_{i=1}^m \gamma_n^{(i)}$$

where $\sigma_{(j)}^{(i)}$ is the posterior variance of $\mathcal{GP} i$ after observing j values. The first inequality in the chain follows from the fact that β_t is increasing, i.e. as $t \leq n$ then $\beta_t \leq \beta_n$. The second inequality follows from the lemmata 5.3 and 5.4 of (Srinivas et al., 2010) where $C = \frac{8}{\ln(1+\sigma^{-2})}$. The third inequality follows from that fact that information gain always increases with each new observation so as $u_i \leq n$ then $\gamma_{u_i}^{(i)} \leq \gamma_n^{(i)}$. We further bound $\sum_{i=1}^m \gamma_n^{(i)}$ by $m\gamma_n$ where $\gamma_n = \sqrt{\gamma_n^{(i)}}$. Afterwards, by Cauchy-Schwarz we get that

$$\sum_{t=1}^n 2\beta_t^{1/2} \sigma_{t-1}^{(i)}(\mathbf{x}_t) \leq \sqrt{mnC\beta_n\gamma_n}$$

Finally, combining the result above with Equation 3 we derive that with probability $\geq 1 - \delta$

$$R_n \leq \sqrt{mnC\beta_n\gamma_n} + \pi^2/6; \quad \forall n \geq 1$$

Here, we have used the fact that $\sum_{t=1}^n \frac{1}{t^2} \leq \pi^2/6 \forall n \geq 1$. \square

B. CaBO vs CoCa-BO

We describe and analyse SCMs used for comparing CaBO with CoCa-BO in this section.

B.1. First Configuration

The SCM that is used for the comparison of CaBO vs CoCa-BO in a scenario where CaBO can achieve the optima is given below:

$$\begin{aligned} \text{Age} &\sim \mathcal{U}(55, 75) \\ \text{BMI} &\sim \mathcal{N}(27.0 - 0.01 \times \text{Age}, 0.7) \\ \epsilon &\sim \mathcal{N}(0, 0.4) \\ \text{Aspirin} &= \sigma(-8.0 + 0.10 \times \text{Age} + 0.03 \times \text{BMI}) \\ \text{Statin} &= \sigma(-13.0 + 0.10 \times \text{Age} + 0.20 \times \text{BMI}) \\ \text{Cancer} &= \sigma(2.2 - 0.05 \times \text{Age} + 0.01 \times \text{BMI} - \\ &\quad 0.04 \times \text{Statin} + 0.02 \times \text{Aspirin}) \\ \text{PSA} &= \epsilon + 6.8 + 0.04 \times \text{Age} - 0.15 \times \text{BMI} - \\ &\quad 0.60 \times \text{Statin} + 0.55 \times \text{Aspirin} + \text{Cancer} \end{aligned}$$

We firstly note that for any values of Age and BMI

$$\begin{aligned} \mathbb{E}[\text{PSA} \mid \text{do(aspirin, statin)}, \text{age}, \text{bmi}] &= \mathbb{E}[\epsilon + 6.8 + 0.04 \times \text{Age} - 0.15 \times \text{BMI} - 0.60 \times \text{Statin} + \\ &\quad 0.55 \times \text{Aspirin} + \text{Cancer} \mid \text{do(aspirin, statin)}, \text{age}, \text{bmi}] = \\ &= 6.8 + 0.4\text{age} - 0.15\text{bmi} - 0.6\text{statin} + 0.55\text{aspirin} + \mathbb{E}[\text{Cancer} \mid \text{do(aspirin, statin)}, \text{age}, \text{bmi}] = \\ &= 6.8 + 0.4\text{age} - 0.15\text{bmi} - 0.6\text{statin} + 0.55\text{aspirin} + \sigma(2.2 - 0.05\text{age} + 0.01\text{bmi} - 0.04\text{statin} + 0.02\text{aspirin}) \end{aligned}$$

It is easy to see that

$$\begin{aligned}
 \underset{\text{aspirin, statin}}{\text{argmin}} \mathbb{E}[\text{PSA} \mid \text{do}(\text{aspirin, statin}), \text{age}, \text{bmi}] = \\
 \underset{\text{aspirin, statin}}{\text{argmin}} -0.6 \text{ statin} + 0.55 \text{ aspirin} - \sigma(22 - 0.05\text{age} + 0.01\text{bmi} - 0.04\text{statin} + 0.02\text{aspirin})
 \end{aligned}$$

In summary, to minimise PSA, Statin should be controlled at its highest value and Aspirin at its lowest value. Since the domains of both variables are $[0, 1]$, the solution of the optimisation problem is Aspirin = 0 and Statin = 1, which is independent of Age and BMI. This implies that the optimal control values for Aspirin and Statin are the same for all values of Age and BMI. This is why the optimum is achievable by CaBO.

B.2. Second Configuration

The SCM that is used for this setup is such that an agent should control Aspirin and Statin based on Age and BMI to achieve the minimum expected value for PSA.

$$\begin{aligned}
 \text{Age} &\sim \mathcal{U}(55, 75) \\
 \text{BMI} &\sim \mathcal{N}(27.0 - 0.01 \times \text{Age}, 0.1) \\
 \epsilon &\sim \mathcal{N}(0, 0.01) \\
 \text{Aspirin} &= \sigma(-8.0 + 0.10 \times \text{Age} + 0.03 \times \text{BMI}) \\
 \text{Statin} &= \sigma(-13.0 + 0.10 \times \text{Age} + 0.20 \times \text{BMI}) \\
 \text{Cancer} &= \text{Statin}^2 + \left(\frac{\text{Age} - 55}{21}\right)^2 \left|\frac{\text{BMI} - 27}{4}\right|^2 + \frac{\text{Aspirin}^2}{2} \\
 \text{PSA} &= \epsilon + \frac{\text{Aspirin}^2}{2} + \left(\frac{\text{Age} - 55}{21}\right)^2 \left|\frac{\text{BMI} - 27}{4}\right|^2 - \\
 &2 \left(\frac{\text{Age} - 55}{21}\right) (\text{Aspirin} + \text{Statin}) \left|\frac{\text{BMI} - 27}{4}\right|
 \end{aligned}$$

If one plugs in the structural equation of Cancer into PSA they get

$$\begin{aligned}
 \text{PSA} &= \epsilon + \text{Aspirin}^2 + \text{Statin}^2 + 2 \left(\frac{\text{Age} - 55}{21}\right)^2 \left|\frac{\text{BMI} - 27}{4}\right|^2 - 2 \times \text{Aspirin} \left(\frac{\text{Age} - 55}{21}\right) \left|\frac{\text{BMI} - 27}{4}\right| - 2 \times \text{Statin} \times \\
 &\left(\frac{\text{Age} - 55}{21}\right) \left|\frac{\text{BMI} - 27}{4}\right| = \left(\text{Aspirin} - \left(\frac{\text{Age} - 55}{21}\right) \left|\frac{\text{BMI} - 27}{4}\right|\right)^2 + \left(\text{Statin} - \left(\frac{\text{Age} - 55}{21}\right) \left|\frac{\text{BMI} - 27}{4}\right|\right)^2 + \epsilon
 \end{aligned}$$

An agent controlling both Aspirin and Statin at $\left(\frac{\text{Age} - 55}{21}\right) \left|\frac{\text{BMI} - 27}{4}\right|$ level achieves the minimal expected value of PSA, namely 0. CaBO fails as it does not consider Age and BMI while controlling Aspirin and Statin.

C. CoBO vs CoCa-BO

C.1. First Configuration

We introduce an SCM such that CoBO which by default controls both X_1 and X_2 based on C is still capable of getting to the optimum value. From the causal graph corresponding to the SCM (Fig. 1a) there are two POMPSes, namely $\langle X_1 \mid C \rangle$

and $\langle X_2 | C \rangle$.

$$\begin{aligned}
 U_1, U_2 &\sim \text{Uniform}(-1, 1) \\
 \epsilon_C, \epsilon_{X_1}, \epsilon_Y &\sim \mathcal{N}(0, 0.1) \\
 C &= U_1 + \epsilon_C \\
 X_1 &= U_1 + \epsilon_{X_1} \\
 X_2 &= |C - X_1| + 0.2U_2 \\
 Y &= \cos(C - X_2) + 0.1U_2 + 0.1\epsilon_Y
 \end{aligned}$$

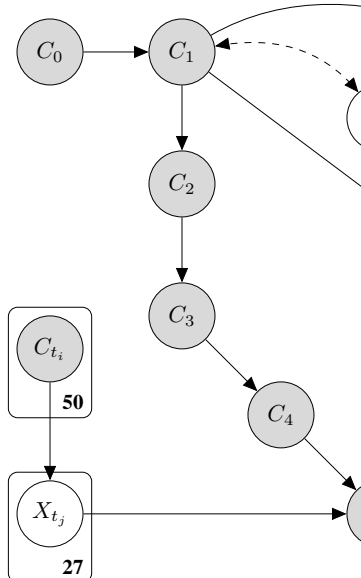
We first note that controlling both X_1 and X_2 is redundant in the sense that controlling X_2 destroys the directed causal path from X_1 to Y rendering the control of X_1 irrelevant to Y . Let X_2 be controlled by an arbitrary function $g : \mathfrak{X}_C \mapsto \mathfrak{X}_{X_2}$. Then the expectation of Y under such control can be expressed as:

$$\mathbb{E}_{\text{CoBO}}[Y] = \mathbb{E}_{\text{CoBO}}[\cos(C - X_2) + 0.1U_2 + 0.1\epsilon_y] = \mathbb{E}_{\text{CoBO}}[\cos(C - X_2)] = \mathbb{E}_{\text{CoBO}}[\cos(C - g(C))]$$

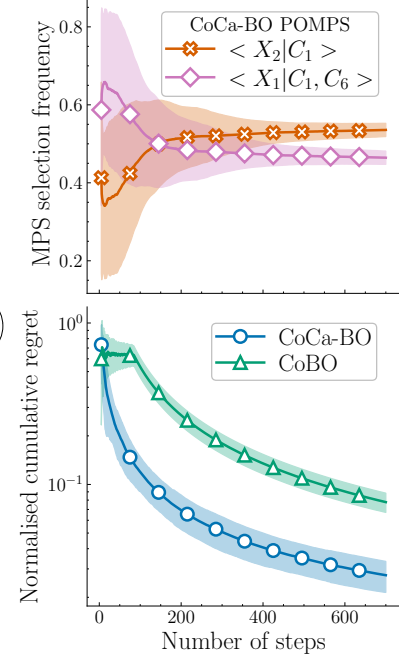
It is trivial to see that to maximise the above expectation one should control X_2 at the value of C , i.e. g is identity. This yields $\max_g \mathbb{E}_{\text{CoBO}}[\cos(C - g(C))] = 1$

Therefore controlling X_2 based on C yields the optimal value as 1 which is the highest value that the expectation of Y may achieve under any policy $\mathbb{E}_\pi[Y] = \mathbb{E}_\pi[\cos(C - X_2) + 0.1U_2 + 0.1\epsilon_y] = \mathbb{E}_\pi[\cos(C - X_2)] \leq 1$. We conclude that CoBO can achieve the optimal value for this SCM.

D. Environment with a large number of variables



(a)



(b) Performance of CoBO and CoCa-BO

Figure 4. (a) A causal graph with a large number of variables. The rectangular nodes represent plates of variables. The number below the rectangles represents the number of variables within each plate. Variables C_{t_i} and X_{t_j} over-specify the environment and are redundant for optimising the expected value of Y . (b) Both methods converge, but CoCa-BO has lower cumulative cost due to smaller policy scopes $\{\langle X_1 | C_1, C_6 \rangle, \langle X_2 | C_1 \rangle\}$.

$$\begin{aligned}
 U_2, U_2 &\sim \text{Uniform}(-1, 1) \\
 C_0 &\sim \mathcal{N}(0, 0.2) \\
 X_1 &\sim \mathcal{N}(U_1, 0.1) \\
 C_1 &\sim \mathcal{N}(C_0 - U_1, 0.1) \\
 C_2 &\sim \mathcal{N}(C_1, 0.1) \\
 C_3 &\sim \mathcal{N}(C_2, 0.1) \\
 C_4 &\sim \mathcal{N}(C_3, 0.1) \\
 C_{t_i} &\sim \mathcal{N}(0, 0.2) \quad \forall i \in \{1, \dots, 50\} \\
 X_{t_j} &\sim \text{Uniform} \left[-1, 1 + 0.1 \frac{\sum_{i=1}^{50} C_{t_i}}{50} \right] \quad \forall j \in \{1, \dots, 27\} \\
 C_5 &\sim \mathcal{N} \left(C_4 + 0.01 \frac{\sum_{j=1}^{27} X_{t_j}}{27}, 0.1 \right) \\
 C_6 &\sim \mathcal{N}(C_5, 0.1) \\
 X_2 &\sim \mathcal{N}(0.5(C_1 + C_6) + X_1 + 0.3|U_2|, 0.1) \\
 Y &\sim \mathcal{N}(\cos(C_1 - X_2) + 0.1U_2, 0.01)
 \end{aligned}$$

This example aims to show that utilising the causal graph may be beneficial even if standard CoBO converges to the optimum. The causal graphs allow the detection and removal of redundancies in policy scopes. This usually leads to policy scopes with a smaller number of variables and improves the convergence in terms of sample efficiency. We use the plate notation (Koller & Friedman, 2009) to display the causal graph which is represented by rectangular nodes in Fig. 4a. This example has purely contextual variables C_{t_i} and X_{t_j} that only influence the rest of the system only through C_5 . It is not necessary to control or observe these variables to achieve the optima. This is reflected in the POMPSes $\{\langle X_1 \mid C_1, C_6 \rangle, \langle X_2 \mid C_1 \rangle\}$ corresponding the causal graph. Both POMPSes contain noticeably fewer variables than the policy scope considered by CoBO $\langle X_1, X_2, X_{t_{1:27}} \mid C_{0:6}, C_{t_{1:50}} \rangle$ where $X_{m:n} = \{X_i \mid m \leq i \leq n\}$. The SCM for this example is defined in terms of stochastic functions for compactness. This has no effect on the proposed work as every stochastic function can be turned into a deterministic one with stochastic inputs (Pearl, 2009d).

One may note that this SCM is similar to the SCM from C.1. Indeed, the structural equations for Y are the same. The same derivations apply to this SCM, proving that CoBO can achieve the optimum. Indeed, Fig. 4b shows that both methods converge to the optimum, yielding a decreasing trend in the normalised cumulative regret. Moreover, CoCa-BO converges faster as it utilises the causal graph and derives policies with a smaller scope. As we see, this significantly improves the convergence speed over CoBO even if it achieves the optimum.

E. Robustness to Noise

We note that the total variance of Y under the optimal policy is actually higher than the variance of ϵ_Y due to an unobserved confounder U_2 , which has a variance of $1/3$. Thus, $\text{var}_\pi(Y) = \frac{1}{3} + \text{var}(\epsilon_Y)$ under the optimal policy π . We emphasize that $\text{var}_{\pi'}(Y)$ under any other policy π' is greater than or equal to $\text{var}_\pi(Y)$.

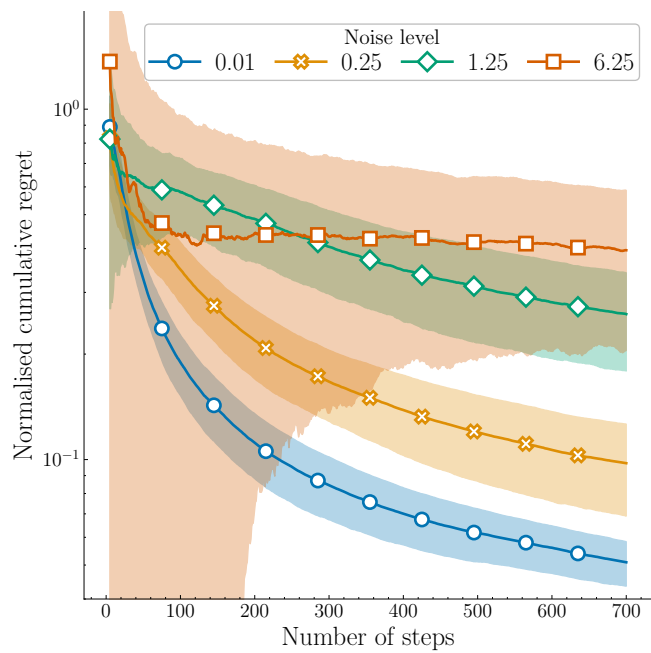


Figure 5. Noise Robustness Analysis: Normalised Cumulative Regret for varying noise levels, evaluated over 700 iterations. The means are shown in solid line while the shaded area shows one standard deviation reported over 110 seeds for each noise level.